Article

The Macroscopic Effect of the Nanofibers Poly (3-Hydroxybutyrate-Co-3-Hydroxy Valerate), plus Aloe vera, or plus Honey, as Scaffolds on the Healing Process of Murine Excisional Wounds

José Manuel Pérez-Galván , José Enrique Hernández-Rodríguez * , José Luis Martín-Barrasa , Maximina Monzón-Mayor , Pedro Saavedra-Santana , Maria-del-Mar Romero-Aleman

Posted Date: 3 June 2025

doi: 10.20944/preprints202506.0228.v1

Keywords: Nanopolymers; Scaffold; PHBV; Aloe vera; Honey bee; electrospinning; tissue engineering; wound healing

 doi:10.20944/preprints202506.0228.v1

Article

The Macroscopic Effect of the Nanofibers Poly (3-Hydroxybutyrate-co-3-Hydroxy Valerate), Plus Aloe Vera, or Plus Honey, as Scaffolds on the Healing Process of Murine Excisional Wounds

José Manuel Pérez-Galván [1], José Enrique Hernández-Rodríguez [2,*], José Luis Martín-Barrasa [3,4,5,6], Maximina Monzón-Mayor [7], Pedro Saavedra-Santana [8] and María del Mar Romero-Alemán [9]

[1] University of Las Palmas de Gran Canaria. Advanced Confocal and Electron Microscopy Research Facility (SIMACE).
[2] University of Las Palmas de Gran Canaria. University Institute for Biomedical and Health Research and Dept. of Nursing.
[3] Animal Facility, Research Unit, Hospital Universitario de Gran Canaria Dr. Negrín, Barranco de La Ballena s/n, 35019, Las Palmas de Gran Canaria, Spain.
[4] IUSA-ONE HEALTH 2 - Sanidad Animal de la Acuicultura y Especies Silvestres, Enfermedades Infecciosas y Seguridad Alimentaria. University Institute of Animal Health and Food Safety (IUSA), University of Las Palmas de Gran Canaria, 35416, Arucas, Spain.
[5] Eukaryotic-Prokaryotic Synergy: Comparative and Translational Medicine (Cardiorespiratory Infectious diseases and Epidemiology group) Fundación Canaria del Instituto de Investigación Sanitaria de Canarias (FIISC), Las Palmas de Gran Canaria, Spain
[6] CIBER de Enfermedades Infecciosas (CIBERINFEC), Instituto de Salud Carlos III, Madrid, Spain.
[7] University of Las Palmas de Gran Canaria. University Institute for Biomedical and Health Research and Dept. of Morphology.
[8] University of Las Palmas de Gran Canaria. Department of Mathematics.
* Correspondence: Hernández-Rodríguez,José Enrique. Joseenrique.hernandez@ulpgc.es.e-mail@e-mail.com; Tel.: (+34 928453458)

Abstract: Background/Objectives: The utility of various biocompatible biological and synthetic polymers has been studied as substrates to provide structural support, facilitate cell migration, and promote the healing of full-thickness wounds by secondary intention. This includes intelligent structures that enable the release of natural products or drugs for these and other purposes. In this study, the primary objective was to analyze and compare, from a macroscopic perspective, the individual behavior of the different polymers in the healing process of a full-thickness skin wound over 40 days in a murine model, in addition to describing the main characteristics of nanofibers and their microscopic ultrastructure.. **Methods**: Two experimental groups were established, PHVB/AV (n=5) and PHVB/Ho (n=5), along with one control group (PHBV) (n=5), all of which underwent biopsies that included the entire thickness of the skin and the panniculus carnosus of the mid-dorsal area of the mouse. Cylindrical pieces of each membrane, measuring approximately 7 x 0.2 mm, were placed in the wound bed and covered with a transparent dressing. No topical treatment was administered during the control process, nor were the implants changed during the healing period. **Results**: Univariate and multivariate analyses were performed. The data show that the PHBV-Ho matrices reduce the diameter of the wounds by 100% after 40 days ($p < 0.001$), compared to PHBV-Av polymers (100%; $p<0.211$) and the control group (68.8%). **Conclusions**: From a macroscopic perspective, the PHBV/Ho polymer significantly accelerated wound healing when applied once to the wound bed, outperforming both the PHBV/AV composite and PHBV alone. Notably, this effect was achieved without the need for dressing changes or additional treatment during the healing period.

Keywords: nanopolymers; scaffolds; PHBV; aloe vera; honey bee; electrospinning; tissue engineering; wound healing

 doi:10.20944/preprints202506.0228.v1

1. Introduction

Several research studies have demonstrated the efficacy of bee honey and Aloe vera in the healing of different skin wounds due to their synergistic physicochemical properties, including antibacterial, anti-inflammatory, antioxidant, [1] and healing process stimulation traits [2–7]. In recent years, several empirical studies have demonstrated that both the single use of these natural products and their combinations with other treatments are effective in treating various types of partial-thickness and full-thickness wounds [4,8–13]. The ability of honey to promote wound healing is a critical factor for this type of scaffold. In a mouse model in vivo treated with honey, the healing and closure rate was better on day 12 compared to a commercial wound dressing, AquacelAg (ConvaTec Inc., Reading, UK)[14].

Hernández-Rodríguez et al. (2023) demonstrated a similar effect of using Aloe and pure honey in a mouse wound healing model without panniculus carnosus over 50 days, mirroring the human wound healing process [15].

The high osmolality and low water (Aw) activity of honey, along with its low pH (3.2–4.5), contribute to these effects [16–20]. Additionally, the presence of organic acids (hexadecanoic, formic, propionic, gluconic, acetic, and benzoic acid), phenolic and flavonoid compounds, as well as the combination of hydrogen peroxide and benzoic acid—which produces very stable peroxide compounds in the presence of endogenous catalase—creates a strong antibacterial effect [9,12,13,16,17,20–29].

In contrast, A. vera, a commercially processed product, has been described as a healing agent for superficial wounds [30–32]. It exhibits angiogenic and anti-inflammatory effects [8,33–36], which favor the proliferation and migration of keratinocytes and collagen deposition, triggering different healing phases and achieving sufficient epithelialization [7,34–38].

Natural and synthetic materials simulate the microscopic organization of the extracellular matrix (ECM), offering structural support and appropriate bioscaffolds for neuritic growth and tissue regeneration [39,40]. ECM nanofibers can be synthesized in either aligned or random networks [41,42]. Alignments and misalignments, as well as fiber diameters, can be controlled depending on the electrospinning parameters, effectively mimicking the structure of the extracellular matrix in various body tissues and organs [40–42].

Several definitions exist for the nanometer scale. The size-based definition typically ranges up to 100 nm but can extend to 1000 nm. The effect-based definition takes into account the physicochemical properties or biological effects, even if the sizes exceed the nanoscale range (up to 1000 nm)[43]. Various studies have shown that both aligned and non-aligned electrospun nanofibers direct neurite extension, with the longest neurites extending parallel to the aligned nanofibers [44,45].

The utility of various biocompatible biological and synthetic polymers as substrates providing structural support for facilitating cell migration and promoting the healing of full-thickness wounds by secondary intention, along with the intelligent structures enabling the release of natural products or drugs for these and other purposes, has been studied [44–48].

The electrospinning technique has been applied to generate scaffolds with nanofibers synthesized from aqueous mixtures of polyvinyl alcohol (PVA) and honey, chitosan and honey, cellulose acetate and honey, polycaprolactone and honey, and silk and honey, creating matrix structures beneficial for wound healing [45–47]. Additionally, the technique is utilized in other regenerative applications [45,48]. However, hybrid nanofibrous scaffolds containing A. vera in combination with polycaprolactone (PCL), collagen, chitosan, and polyvinyl alcohol (PVA) have been evaluated as potential biomaterials for skin regeneration [47–49]. Moreover, PHBV/collagen nanofibers and PHBV microspheres were employed as scaffolds for PC12 cells [44,45]. The tissue response to polymeric implants of poly (3-hydroxybutyrate-co-3-hydroxy valerate) [PHBV] in biopsies of scarless skin regeneration was similar to the reaction to silk and less pronounced than the response to other scaffold PHBV sutures implanted intramuscularly for over a year. It did not induce an acute response at the implantation site [40,50–52].

 doi:10.20944/preprints202506.0228.v1

However, no studies, including ours, have utilized a combination of hybrid scaffolds composed of PHBV, honey, or A. vera for wound healing, to create a molecular structure that simulates the extracellular matrix as structural support for tissue regeneration [53].

These scaffolds act as implants inserted into the wound bed without needing to be changed during the healing process. The technique used to create wounds that heal by secondary intention, similar to human skin, was that described by Davison (2013) [54] and Ren (2012) [55]. They inserted a subcutaneous silicone ring into the dorsal area of the mouse and generated a wound by performing a biopsy of the entire thickness of the skin, including the carnosus panicles in the central region of the ring. Later, they sutured the upper edges of the wound to the inner edge of the wound, thus preventing rapid closure due to the action of the carnosus panicles, a skeletal muscle layer found in the skin of mice that facilitates wound healing by contraction. Without this layer, a secondary intention wound closure effect similar to that in human skin would be achieved.

In this study, the aim was to analyze and compare, from a macroscopic point of view, the individual behaviour of different polymers such as PHBV, honey bee, or A. vera, in the healing process of a full-thickness skin wound over 40 days, in addition to describing the main characteristics of nanofibers and their microscopic ultrastructure.

2. Materials and Methods

Animals

In accordance with the proposal to reduce the number of animals required without compromising statistical significance [15,56,57] eight-week-old male CD15 Swiss mice (n = 15), averaging 41.2 g in weight, were randomly selected for experiments. The mice were housed in individual cages with unrestricted access to food and water dispensers. They were cared for according to the European Directive 2010/63/EU on the protection of animals used for scientific purposes [57]. The animals were randomly divided into two experimental groups and one control group of five animals (n=5) per group.

The Animal Ethics and Well-being Committee of the University of Las Palmas de Gran Canaria (ULPGC) approved the experimental procedures (Ref. 004/2013CEBA ULPGC).

Before and after the surgical procedure, the weight of the mice was measured. Glycemia was assessed using a standard glucometer (FreeStyle Optium Neo de Abbott®) with a sample extracted from the lateral tail (coccygeal) vein. Body temperature was recorded with an infrared thermometer (TZL-801A), and the diameter of the wound was gauged with a manual Vernier© caliper. These measurements were complemented by images captured from a tripod at the same distance using a smartphone (Samsung S5) camera, while the animals were positioned on millimeter graph paper for scale. Observations were conducted at various time points ([t0]: immediately following surgery, [t7]: 7 days, [t15]: 15 days, [t20]: 20 days, and [t40]: 40 days) [15,34,58–60] by measuring the size of the wounds based on the average of two measurements taken perpendicular (d1) and parallel (d2) to the mouse's backbone. Consequently, 20 observations were made per mouse, totaling 260 observations (Supplemental Data, Table S3).

Additionally, we assessed if the granulation tissue was pink and clean, if the wound bed showed total or partial slough or cellular debris, and if the wound exhibited complete closure covered by epithelial tissue with plentiful hair follicles.

Images were analyzed with the image analysis software package ImageJ®[61].

Surgical procedure

The animals were anesthetized intraperitoneally with 0.03 mL of medetomidine (1 mg/kg; 0.03 mg) and 0.06 mL of ketamine (100 mg/kg; 3 mg). For revival, 0.01 mg/kg of atipamezole was administered. Tramadol was given ad libitum (25 mg/kg) orally [62].

A small, sterile subcutaneous nitrile ring (10 mm in diameter, fig. 1 and fig. 2.A) was inserted into the dorsal area of the animals and securely fixed subcutaneously in each animal to study the tissue repair mechanisms related to this type of wound and to regulate and control the contraction occurring in the skin of these animals during healing [15,54,55].

 doi:10.20944/preprints202506.0228.v1

Ten days after insertion, a full-thickness wound was created on the skin within the ring, including the panniculus carnosus, using the same anesthetic procedure described above. A sterile skin biopsy punch (8 mm in diameter) was used (Ref. 94158BP-80-FA) (fig. 1 and fig. 2.B). The internal edge of the ring was sutured to secure the wound and prevent skin contraction, following the experimental models of Davidson et al. (2013)[54], Ren et al. (2012)[55], and Hernández-Rodríguez et al. (2023)[15] (fig. 2.C). Thus, the model simulates the biological processes of human wound healing.

Scaffold Fabrication and Morphological Characterization

Electrospinning is a versatile method for producing polymeric nanofiber scaffolds. A high voltage is applied between the metal needle and the collector, while the polymer solution is pumped through a syringe. The polymeric droplets are stretched and ejected onto the collector via electrostatic repulsion. During the ejection process, the solvent evaporates, allowing the solid fibers to reach the collector [63,64].

In our experiment, we fabricated three different non-aligned nanofibers from poly(3-hydroxybutyrate-co-3-hydroxyvalerate) (Sigma-Aldrich, Prod. N.º 403121, CAS N.º: 80181-31-3) [PHBV] scaffolds. The first is PHBV (control). The other scaffolds were created by mixing PHBV with natural components of A. vera (Aloe puro en biogel 99%. Cultivo ecológico. Aloe Park Tenerife. Luciano Reverón e hijos S.L.) (PHBV/Av) and honey (Miel pura multifloral de Abejas, Cuevas de Guayadeque, Ingenio, Gran Canaria. Registro Sanitario N º: E23.03229/GC/CEE) (PHBV/Ho). The manufacturing parameters for these scaffolds can be found in the corresponding published patents, EP 3428117[65] and EP 3461788 [66]. The circular membranes have a diameter of 7 mm and a thickness of 0.2 mm.

he surface morphology of the scaffolds was examined using a field emission scanning electron microscope (FESEM), specifically the Zeiss Sigma 300VP, at the electron microscope (EM) facility of the University of Las Palmas de Gran Canaria (SIMACE Facility). Samples were attached to cylindrical aluminum stubs with double-sided carbon adhesive tape and subsequently observed with the FESEM using the secondary electron detector at very low voltages, which ranged from 0.8 to 1.5 kV. Representative images of each matrix's topography were captured at various magnifications.

Control and Experimental Treatments

Each membrane piece, approximately 1 cm in diameter, was sterilized by irradiation with a commercial ultraviolet (UV) germicide lamp (λ = 254 nm) at a distance of 25 cm for 35 minutes [67]. The wounds in the first group (n=5) were treated with saline (SF) or PHBV polymers only. This group served as the control.

The polymer scaffold PHBV/Av served as the second experimental group (n=5), while the third experimental group (n=5) was treated with the scaffold PHBV/Ho.

No topical treatments were applied, nor were any modifications made to the scaffolds during the control process. The wounds of the experimental groups were covered with a Tegaderm® transparent dressing (Fig. 1). Observations were recorded at different time points ([t0]: immediately following surgery, [t7]: 7 days, [t15]: 15 days, [t20]: 20 days, and [t40]: 40 days), and measurements were taken for weight, temperature, glycemia, and wound size (Fig. 2.D-O).

Data were quantified with ImageJ® software (NIH, USA) [68] and analyzed statistically.

Histological Analysis

Regenerated tissues were sectioned in four equal parts each, fixed in Zamboni's fixative, and stored in an ultra-freezer at -40°C. Sample sections were selected for semithin optical microscopy.

Samples pre-treatment for semithin sections were as follows: samples were washed in phosphate buffer saline (PBS) and fixated with glutaraldehyde, 2,5% (Electron Microscopy Sciences – EMS, Glutaraldehyde 25%, EM grade, 16220) overnight, washed twice with PBS, and post-fixed with 2% osmium tetroxide (EMS, 19170) for 3 hours. They were dehydrated with a graded series of ethanol (20, 40, 60, 70, 96, and 100%). They were immersed with a mixture of pure ethanol and propylene

 doi:10.20944/preprints202506.0228.v1

oxide (EMS, 20401) (1:1, v/v); propylene oxide; propylene oxide and Embed812 epoxy resin (EMS, 14120) (1:1, v/v), and pure epoxy resin overnight. Semithin (1 µm) sections were performed under a Leica ultramicrotome EM UC7. As standard procedure for staining semithin sections Toluidine Blue (TBb) (Panreac, 251176) was used. Also, a polychromatic staining methods was used: Toluidine Blue-Basic Fuchsine (Sigma Aldrich, 215597) (TBb/BFb).

Semithin sections images were acquired using an optical microscope, ZEISS Axio A1, Carl ZEISS, at SIMACE.

Statistical Analysis

Univariate analyses. The percentage variations in wound surfaces between the first and last days were summarized as medians and interquartile ranges (IQR = 25th–75th percentiles). Multiple comparisons among the treatments were conducted using nonparametric methods.

Multivariate analysis. Multivariate analysis was used to evaluate the effect of the treatments on the wound surface on each control day, which was ultimately adjusted for weight, temperature, and glycemia level. Since the design employed a repeated measure, the data were analyzed using mixed models. The wound surface was transformed logarithmically. Thus, we denoted $Wound$ by "mouse, treat. day" and the wound surface for the mouse by "$mouse$" receiving the treatment "$treat$" at day "day." According to Laird and Ware (1982) [69], we considered the following mixed model:

$$Log\ wound\ (mouse, treat.day) = \theta + \tau(treat) + \beta.day + \sum_{k} \gamma k.Zk + mouse + e\ (mouse, treat.day)$$

Here, τ_{treat} denotes the treatment effect ($\tau_{reference} = 0$); $mouse$ is the random effect of the mouse, which we assume is usually distributed with mean zero and standard deviation σ and $(mouse, treat.day)$ is the error term. In the analysis, the covariables weight, temperature, and glycemia level were introduced. Next, variables were selected based on the Akaike Information Criterion (AIC) [70].

Therefore, we denoted the variables by $_k$ that were finally maintained in the model after the selection. The model was estimated using the restricted maximum likelihood and summarized as coefficients, standard errors (SE), and p-values.

Statistical significance was established at $p < 0.05$. Data were analyzed using the R package version 3.1.1 [71].

3. Results

3.1. Animals

The parameters of weight, temperature, and blood glucose levels were consistent across the three groups of animals. The final sample included 8-week-old animals (n = 13) with an average weight of 41.4 g (SD: 3.1). Two animals were excluded from the Aloe experimental group because they could not tolerate the inserted ring. Figure 1 shows the protocol followed with the animals, and Figure 2 illustrates the evolution of wound size in relation to the type of polymer applied and the number of control days. The PHBV/Ho experimental group demonstrated better efficacy in terms of healing time compared to the control group and the other experimental groups (PHBV/Av).

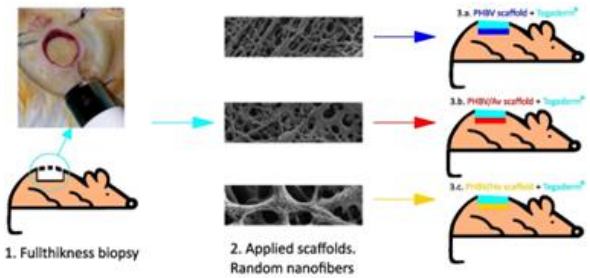

Figure 1. Protocol.

 doi:10.20944/preprints202506.0228.v1

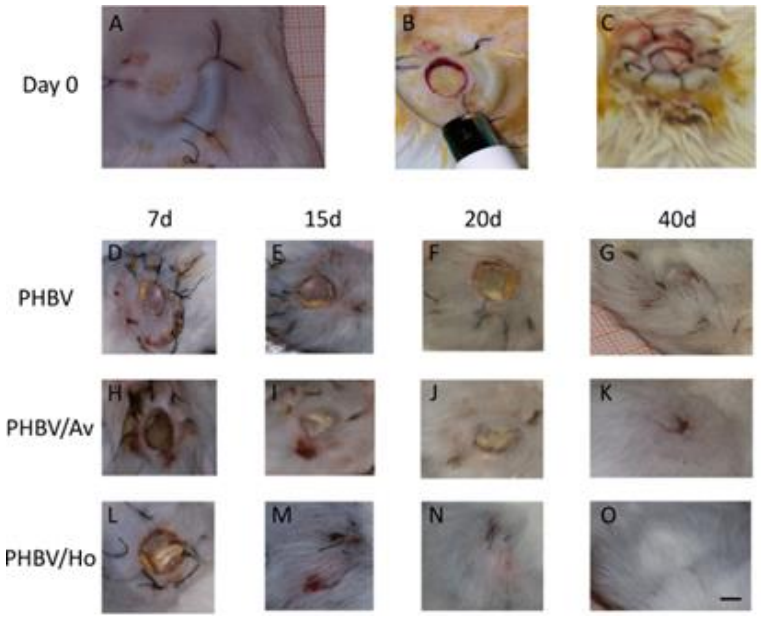

Figure 2. Anatomical views of the dorsal skin of mice during the surgical procedure (A-C) and representative images of the wound healing process at 7, 15, 20, and 40 days of treatment with PHBV only, dressing (D-G), PHBV + commercial Aloe vera (PHBV/Av) (H-K), and PHBV + natural honey (PHBV/Ho) (L-O). The rostral side of the animals is oriented upwards in all images. (A-C) Note the subcutaneous nitrile ring (8 mm diameter) before the removal of the full-thickness skin using a trucut (B). The nitrile ring was secured with additional sutures prior to the initiation of the corresponding topical treatment (C). (D-G) Observe the very slow and uneven progress of wound healing in the PHBV (control) group, which displayed a friable wound bed at 15 to 20 days. The wound remained open at 40 days postlesion (G). The PHBV/Av group showed a gradual decrease in wound size (H-J); however, healing was not complete. The PHBV/Ho group exhibited a more dynamic wound healing process (L-O) compared to the other groups, with ulcers containing granulation tissue at 15 days (M) nearly healed at 20 days (N) and fully healed by 40 days (O). Note that the wound was closed and covered by several hair follicles at 40 days postlesion (O). Animals were imaged on laminated millimeter grid paper for scale reference. The scale bar in R (5 mm) applies to all images.

Wound evolution was slow and highly irregular from day 7 in the control group (PHBV). A friable wound bed was observed on day 15, characterized by the absence of discharge and the formation of an incomplete skin surface with a rigid appearance (fig. 2.D-G). Moderate hair follicles were noted in a partially healed area on day 40 (fig. 2.G). The average sizes of the wounds for this group were 7.5 mm and 5.8 mm, respectively, on days 7 (t7) and 15 (t15) (fig. 2.D-E), 4 mm on day 20 (t20) (fig. 2.F), and 2.4 mm on day 40 (t40) (fig. 2.G). The average weight was 38.6 g, glycemia was 122.24 mg/dL, and temperature was 34.5 °C.

The size of the wound in the PHBV/Av experimental group gradually decreased (t7 = 7.2 mm; t15 = 5.9 mm; t20 = 5 mm; t40 = 1 mm), showing better results than the control group, although the wound had not fully healed by day 40 (fig. 2.K). The wound bed exhibited an incomplete skin surface with a rigid appearance (fig. 2.H-K). The average weight of the animals was 44.8 g, the average temperature was 34.5 ºC, and the average blood glucose level was 126 mg/dL.

We observed a gradual reduction in the initial average diameter of the scars during the progression of the wounds treated with PHBV/Ho (fig. 2.L-O), beginning on day 7 (t7 = 7.9 mm) (fig. 2.L) and continuing steadily through days 15 (t15 = 5 mm) and 20 (t20 = 2.4 mm) (fig. 2.M-N). From day 15 to day 20, there was no secretion, and the wound bed remained clean and free of exudate (fig. 2.L-N), with abundant hair follicles visible in the healed areas (fig. 2.O). The average weight was 41 g, the average temperature was 34.1 °C, and the blood glucose level was 137 mg/dL.

3.2. Scaffold Fabrication and Morphological Characterization

 doi:10.20944/preprints202506.0228.v1

Representative figures of the macroscopic view of the scaffolds are shown in Figure 3.A. Figure 3.B represents the PHBV (control) surface under FESEM. Figures 3.C and 3.D, PHBV/Av scaffold and PHBV/Ho, respectively, under FESEM.

All three scaffolds comprise a disordered and intricate network of nanofibers with interconnected voids resembling a 3D porous network. Scaffolds PHBV (fig. 3.B) and PHBV/Av (fig. 3.C) display smooth and homogeneous nanofiber surfaces characterized by their characteristic pearls. The addition of Aloe results in fibers very similar to those of PHBV. It has been reported for a blended hybrid poly (vinyl alcohol)/Aloe vera/Chitosan that the inclusion of Aloe [72] creates a topography quite different from that observed in PHBV/Av. However, the incorporation of natural honey, PHBV/Ho (fig. 3.C), completely alters the surface morphology, resulting in an irregular topography with "nano-bubbles" surrounding the nanofibers (fig. 3.D, blue arrows).

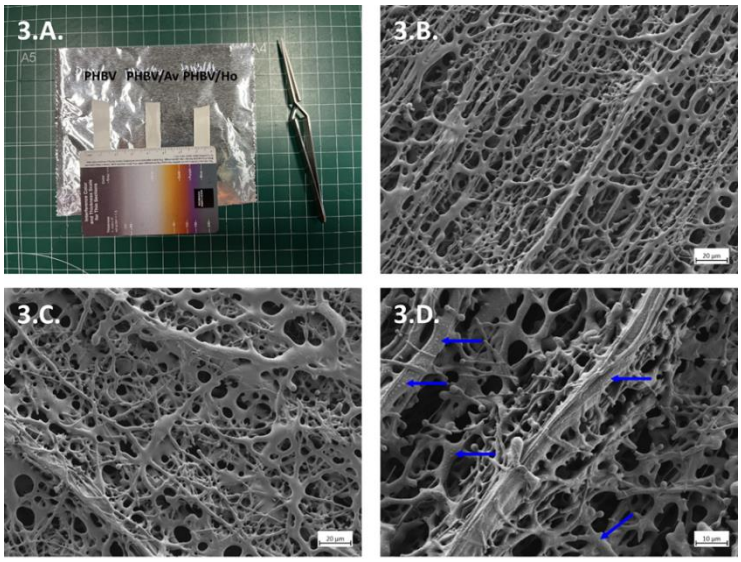

Figure 3. Ultrastructure of non-aligned PHBV nanofibers: 3.A.Scaffolds, macroscopic view; 3.B: PHBV;.3.C: PHBV/Av under FESEM; 3.D:PHBV/Ho under FESEM.

3.3. Histology

Figure 4.A. represents a panoramic view of a semithin section of skin control (no treatment), and representative figures of the biopsies with the scaffolds are shown in Figure 4.B-D: PHBV (Figure 4.B), PHBV/Av (Figure 4.C.) and PHBV/Ho (Figure 4.D.).

Light microscopy does not detect the presence of polymers in the biopsies. Furthermore, no foreign bodies were observed in any of the processed specimens, suggesting their possible presence/rejection by the animal's skin. A plausible hypothesis is that over the course of the 40-day experiment, the polymer was completely reabsorbed, leaving no trace. These data will need to be corroborated by transmission electron microscopy (TEM) observation of the ultrastructure of the biopsies.

The skin structure appears to be reconstructed when examined biopsies with the different scaffolds (PHBV, PHBV/Av, and PHBV/Ho), as the three layers (epidermis, dermis, and hypodermis) are clearly visible. The structure of the epidermis, Figure 4. B.1-D.1, appears to be fully and free of morphological defects. In the same figure, in the dermis area, the following can be distinguished: hair bulb (Hb), connective tissue (CT), glands (Sg), and fibroblasts (F).

On the contrary, significant differences are observed in the hypodermis layer, Fig. 1 B.2 to D.2, compared to the control. In the PHBV biopsies, Figure 4.B.2, the structure of this layer is not well defined: the adipose tissue layer is almost nonexistent and appears to be in its primitive phase: very few adipocytes and very small in size. The hypodermis in the PHBV/Av biopsy samples, Figure 4.C.2, presents a very irregular layer, with scattered convective tissue and some areas with gray adipose tissue. No white adipose tissue is observed. Finally, the hypodermis of the PHBV/Ho biopsies, Figure

 doi:10.20944/preprints202506.0228.v1

4-D.2, presents a state similar to that of healthy skin: white and gray adipose tissue can be seen, as well as the loose connective tissue characteristic of this layer.

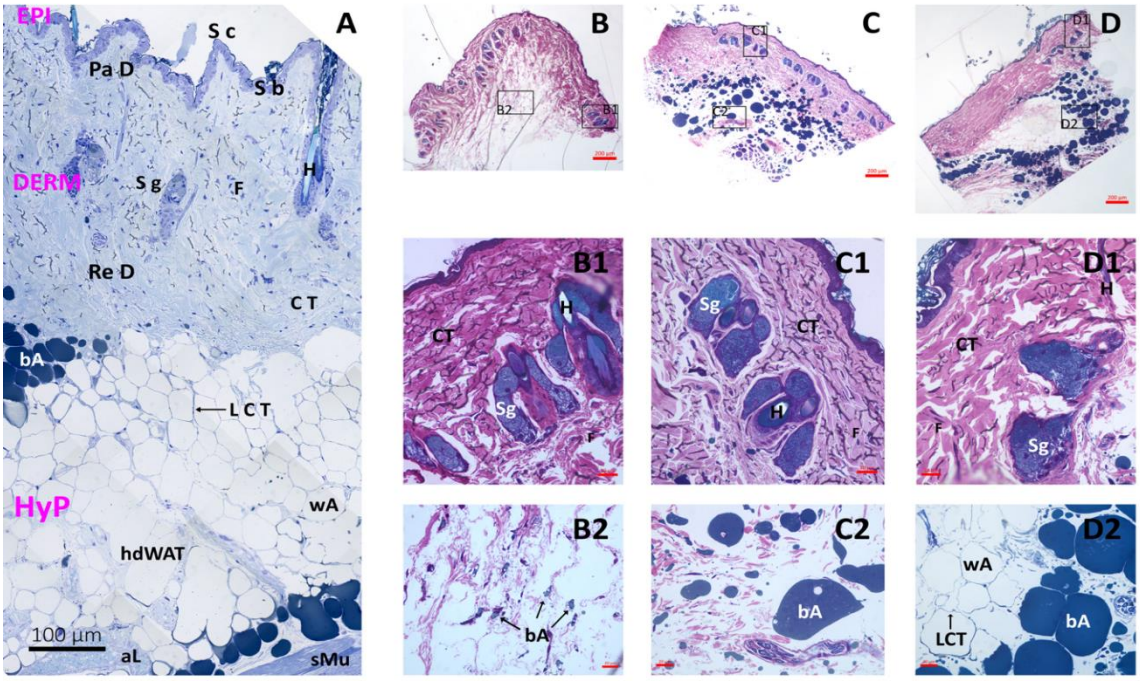

Figure 4. Semithin sections. (A) Biopsy control. Panoramic view. (B) Biopsy with scaffold PHBV. Panoramic view. (B1) Detail of B, Epidermis and Dermis. (B2) Detail of B, Hypodermis. (C) Biopsy with scaffold PHBV/Av. Panoramic view. (C1) Detail of C, Epidermis and Dermis. (C2) Detail of C, Hypodermis. (D) Biopsy with scaffold PHBV/Ho. Panoramic view. (D1) Detail of D, Epidermis and Dermis. (D2) Detail of D, Hypodermis. Legend. A: Adipocytes, (bA: Brown Adipocyte, wA: White Adipocyte); C T: Connective Tissue (Dense irregular); DERM: Dermis; EPI: Epidermis; F: Fibroblasts; H: Hair; Hb: Hair bulb; HyP: Hypodermis; hdWAT: hypodermis White Adipose Tissue (Unilocular adipocytes); L C T: Loose Connective Tissue; Pa D: Papillary Dermis; Re D: Reticular Dermis; S g: Sebaceous glands (Irregular saccular); sMu: striated Muscle.

3.4. Statistical Analysis

Table 1 shows the variation in the wound surfaces from the first to the last day. This percentage reduction was complete in the PHBV/Ho group. Table 2 shows that the PHBV/Ho polymer treatment significantly differed from the PHBV polymer treatment alone ($p < 0.001$). The difference between honey and *A. vera* treatments was quasi-significant ($p = 0.0628$).

Table 1. Variation in wound surfaces from the first day to the last day.

Treatment	Day 0(first)	Day 40(last)	Percent reduction*
PHBV	8(8,8)	2,5(2.5,3.2)	68.8(60,68.8)[a]
PHBV + Honey	8(8,8)	0(0,0)	100(100,100)[b]
PHBV + Aloe Vera	8(8,8)	0(0,1)	100(87.2,100)[a,b]

Data are presented as medians (interquartile range [IQR]). (*) Different superscripts indicate significant differences at $p < 0.05$.

Table 2. A mixed model for the surface of deep injuries (logarithm scale) using PHBV as a control.

 doi:10.20944/preprints202506.0228.v1

	Coefficient (SE)	p-value
Intercept Treatment	2.334(0.085)	<0.001
PHBV(reference)	0	-
PHBV + Honey	-0.382(0.107)	<0.001
PHBV +Aloe Vera	-0.136(0.109)	0,211
Time, per day	-0.054(0.004)	<0.001

Figure 5 indicates that the most significant reduction in wound surface evolution was associated with treatment using PHBV/Ho.

Glycemia levels and temperature were not statistically significant and, therefore, were not included in the model.

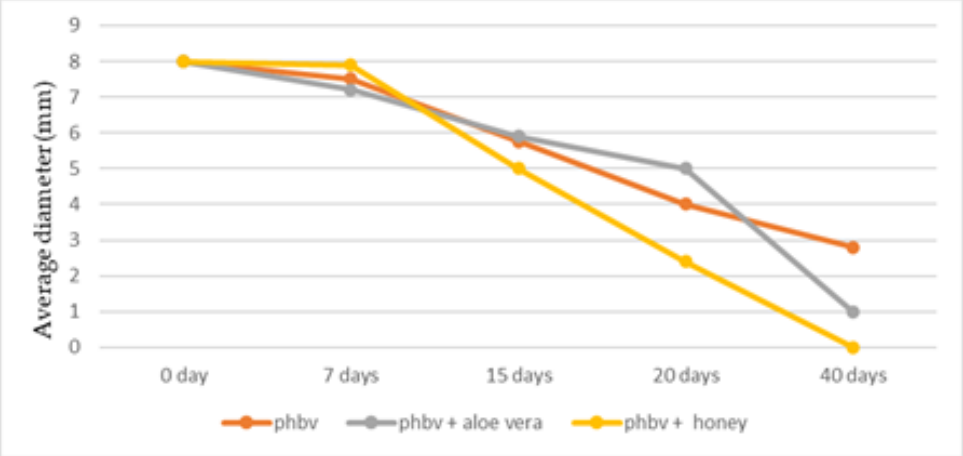

Figure 5. Evolution of wound size according to the polymers used in treatment and the number of treatment days.

4. Discussion

The insertion of the subcutaneous ring in the dorsal area of the mouse's skin allowed for long-term monitoring of the evolution of the wound in the study of the healing process by secondary intention similar to that which occurs in human skin (Davidson et al., 2013 and Ren et al., 2012)[54,55], and is therefore shown to be an appropriate method for in vivo clinical monitoring of this process in murine models.

This study presents evolution data extending beyond the standard 7 to 15 days [52,56,57,64] up to 40 days [15] for excisional wounds in mice. The wound healing in the control group differed significantly from that in the two experimental groups. Overall, the quality of scar tissue in the honey group on day 40 was better than that in the A. vera group. In contrast, the quality was poorer in the control group.

In this regard, Rubiano-Navarrete et al. (2024) and Abrigo et al. (2014) highlight the utility of electrospun nanofibers as effective structures for promoting chronic wound healing [53,78].

Moreover, several authors have highlighted the effectiveness of using these scaffolds along with various products to achieve complete healing in full-thickness wounds [41,42,46–49,53,75–77,79,81].

Pilehvar-Soltanahmadi et al. (2018) indicate that incorporating natural substances into nanofibers through electrospinning techniques creates fibers that enhance the healing process by both providing a substrate for cellular support and enabling the in situ release of these products into the ulcerous niche. This approach yields better results than using only the polymer without these added

 doi:10.20944/preprints202506.0228.v1

natural components, as their various properties directly influence the healing process by stimulating angiogenesis, promoting fibroblast production (effects of honey), or facilitating collagen remodeling (effects of aloe vera)[79].

Similarly, the potential to synthesize the polymer in a reticular or aligned manner ensures dual functionality, enabling granulation tissue regeneration with the non-aligned form and promoting neuritic regrowth with the aligned form. Masaeli et al. (2013) and Prabhakaran M. et al. (2013) demonstrate the effectiveness of electrospun aligned PHBV/collagen nanofibers as substrates for nerve tissue engineering, indicating that these aligned fibers allow neurite regrowth [43,46].

Masaeli et al. point out the promising possibilities of using aligned PHBV nanofiber composites for nerve regeneration if compounds that stimulate this growth are added [43].

In this regard, Romero-Alemán et al. (2019, 2025) found that the use of aligned and non-aligned PHBV matrices, combined with aloe vera and honey, promotes neurite regrowth as well as the regeneration of mouse skin after wounding [41,42].

Furthermore, the polymer's characteristics aid in managing the water produced by honey's osmotic action, evenly distributing it across the membrane's surface. This process ensures that an optimal moisture level is maintained for effective healing and cell adhesion [39–41,45,47,48,53].

In our study, we observed that wounds treated with nanofibers incorporating the natural compounds aloe vera and honey produced better results than those treated with the polymer alone. Additionally, we noted that wounds treated with PHBV polymer and honey healed more quickly than those treated with PHBV polymer and aloe. In a study by Hernández-Rodríguez et al. (2023), it was found that using these natural products in their pure form for wound healing yielded different outcomes, with better healing dynamics noted with aloe than with honey, compared to traditional hydrocolloid dressings [15]. However, this study found that when these natural products were combined with the PHBV polymer, the healing dynamics were significantly more favorable with the polymer combined with honey than with aloe or the polymer alone.

The properties of honey, when combined with those of the polymer, create a synergistic effect, allowing honey's attributes (anti-inflammatory, antimicrobial, fibrinolytic, osmotic, and tissue regenerative) to enhance the polymer's ability to absorb excess moisture due to its hydrophilic nature. This helps maintain an appropriate moisture level that prevents the wound edges from macerating and allows the stem cells at the edges to continue the skin repair process [15,40,48–50].

This polymer combination of PHVB and honey fosters quicker wound healing under improved conditions compared to the polymer made from aloe vera and the control polymer alone, as illustrated in Figure 4.

It is important to note that human skin takes approximately 60 to 90 days to heal, depending on various factors [83,84]. Therefore, utilizing this combination of PHBV polymer and honey may be an intriguing strategy to explore for enhancing the healing of secondary intention wounds and chronic wounds [53,77–80,84,85].

Furthermore, glycemia levels, temperature, and weight parameters were within physiologically normal limits [73].

Forty days after lesioning, scaffolds containing honey and A. vera accelerated wound closure. The most significant differences in wound diameter among the groups were observed at 20 and 40 days post-lesion (Fig. 2.D-O). Consequently, the PHBV/Ho group exhibited enhanced dynamic wound healing (Fig. 2.L-O).

The compounds of the PHBV/Ho and PHVB/Av nanofibers will be released in a controlled manner, promoting cell growth. Scaffolds with honey contributed to faster healing than the others, as observed in the image sequence and graphics (Fig. 2.A-O; Fig 5). As other authors have described, this may be linked to the antibacterial and granulation tissue promotion properties of honey [9,12,26,27,29]. The enzymatic and autolytic properties of honey [13,19,24] eliminate cellular debris by activating plasmin and proteases, enabling the digestion of fibrin layers adhering to the wound bed and facilitating the healing process, as demonstrated in a study by Hernández-Rodríguez et al., (2023) [15]. This process is supported by the web-like arrangement of the fibers, leading to the

 doi:10.20944/preprints202506.0228.v1

development of active granulation tissue, which results from previous angiogenesis, fibroblast migration, and collagen deposition [73,74].

The scaffold PHBV is a polyester derived from polyhydroxyalkanoate produced by microorganisms under unbalanced growth conditions [40]. It possesses desirable properties, including a high surface-area-to-volume ratio, adequate mechanical stability, and sufficient pore size in the resulting nanofibrous scaffolds. The high porosity of this nanofiber enables oxygen and water permeability, as well as nutrient exchange. It effectively removes metabolic waste and prevents fluid accumulation at the wound site since nanofibrous dressings absorb wound exudates much more efficiently than film-type dressings. Hence, the porous structure allows appropriate permeation of atmospheric oxygen into the wound [40,74,75,78]. Additionally, high surface areas foster the attachment of fibroblasts and endothelial cells, along with their subsequent proliferation and differentiation during tissue regeneration [40,48,49,74–76,78]. Contact with blood activates the coagulation and complement systems, which is essential as it stimulates the initial phase of wound healing [59]. In our study, PHBV/Av and PHBV/Ho scaffolds seem to provide a favorable scaffold for cell proliferation, as suggested by the previously cited authors [40–43,47–49,74–79,81].

On the other hand, the authors [40,74–78] demonstrated that this type of PHBV nanofiber provides an excellent structure for the attachment and growth of chondrocytes as a cell culture surface for tissue engineering. This material did not cause any acute vascular reactions or adverse events at the implantation site, such as suppurative inflammation or necrosis, as shown in fig. 2. Its degradation into oligomers and monomers is not toxic to cells [40]. The degradation of these fibers likely occurs after the microcapsules release various compounds [40,75,76,78–80]. In our case, the microcapsules may have released different honey and A. vera compounds, facilitating the wound-healing process.

The PHBV/Ho group showed faster dynamic healing compared to the PHBV/Av group, with a gradual reduction in wound size (Fig. 2.L-O) until complete healing at 40 days. However, healing in the PHBV/Av group remained incomplete at 40 days (Fig. 2.K). In the PHBV group (control group), the degree of wound healing showed uneven and prolonged progression, resulting in a friable ulcerative bed at 15–20 days. The wound in this group remained open 40 days after injury (Fig. 2.G). This is illustrated in the histological images in Figure 4, which show healthy skin with a more organized basal structure in the PHBV/Ho biopsy samples (Fig. 4-D.2). In contrast, the other biopsies reveal a less organized subcutaneous structure compared to that of the honey polymer (Fig. 4-B.2 and C.2).

The most important achievement of this experiment was that the scaffold was placed only once, and no other significant treatment was performed on the original scar, which was sufficient for wound healing. Furthermore, without replacing the scaffold, after 40 days (approximately 5 weeks), this hybrid honey scaffold achieved complete wound healing by maintaining an adequately humid environment necessary for the healing processes, according to Pilehvar-Soltanahmadi et al. (2018) [79].

Our patented scaffolds, PHBV/Av and PHBV/Ho, infused with natural products, can maintain wound moisture and thereby support the contraction of autologous skin. Additionally, fluid and cell infiltration promote structural degradation and scarless remodeling (see Fig. 4B1, 4C1, 4D1), present study) [80–82].

Therefore, they can have biomedical applications such as designing graft materials, coating endoprostheses and surgical meshes to enhance cell growth and adhesion, reinforcing sutures in poorly vascularized cartilaginous tissues, and serving as implants in ulcerated tissue due to dependency, including dental implants or coatings, wound dressings, and absorbable sutures, as suggested by different authors [41,42,47–49,75–82].

5. Conclusions

In conclusion, the PHBV/Ho scaffold proved more effective than the control PHBV in reducing wound size without alteration during the experiment. Hybrid A. vera and honey scaffolds may serve

 doi:10.20944/preprints202506.0228.v1

as useful platforms for cell migration. Additionally, they accelerate wound healing, promote scar-free skin regeneration with appendage recovery, and may aid in axonal regrowth, as observed in a mouse model of human skin ulcers.

From a macroscopic perspective, the PHBV/Ho polymer significantly accelerated wound healing when applied once to the wound bed, outperforming both the PHBV/AV composite and PHBV alone. Notably, this effect was achieved without the need for dressing changes or additional treatment during the healing period, suggesting its potential for biomedical applications.

6. Patents

Due to this research, the following patents were applied for and obtained:

1. Monzón, M., Romero, M., Hernández, JE., Pérez, JM. Hybrid Aloe vera nanofibers. European Patent Office. EP 3461788;12.10:2022. Munich.

2. Monzón, M., Romero, M., Hernández, JE., Pérez, JM. Hybrid honey nanofibers. European Patent Office. EP 3428117;27.07:2022. Munich.

Supplementary Materials: The following supporting information can be downloaded at the website of this paper posted on Preprints.org, Table S1: Supplementary data.

Author Contributions: Conceptualization, H.R.J.E., R.A.M.M; P.G.J.M. and M.M.M.; methodology, H.R.J.E.P.G.J.M., and M.B.J.L.; software, P.G.J.M.; validation, M.B.J.J, R.A.M.M., and M.M.M..; formal analysis, S.S.P.; investigation, H.R.J.E, and M.B.J.L.; resources, H.R.J.E., P.G.J.M.. and M.B.J.L; data curation, H.R.J.E., M.B.J.L., and S.S.P.; writing—original draft preparation, H.R.J.E.; writing—review and editing, R.A.M.M., P.G.J.M., and M.M.M; visualization, H.R.J.E., R.A.M.M.,P.G.J.M., and M.M.M.; supervision, H.R.J.E., and M.B.J.L..; project administration, H.R.J.E., and R.A.M.M.; funding acquisition, R.A.M.M., and H.R.J.E.. All authors have read and agreed to the published version of the manuscript.

Funding: This research was funded by Consejería de Educación del Gobierno de Canarias (SolSubC200801000281); Universidad de Las Palmas de Gran Canaria (ULPGC2013-12); Agencia Canaria de Investigación, Innovación y sociedad de la Información (CEI2018-34); Cabildo Insular de Gran Canaria (C2016/39; C2017/100) and Mancomunidad del Sureste de Gran Canaria (C2017-13; C2018-23).

Institutional Review Board Statement: The animal study protocol was approved by the Animal Ethics and Wellbeing Committee (CEBA) approved the experimental procedures at the University of Las Palmas de Gran Canaria (Ref 004/2013CEBA ULPGC).

Informed Consent Statement: Not applicable.

Data Availability Statement: The data for this research can be found in Table S1, supplementary data.

Acknowledgments: The authors thank the technicians Noelia Guedes, Susana Zambrano, and Juan Francisco Arbelo for their excellent technical assistance. We also thank the Advanced Confocal and Electron Microscopy Research Service (SIMACE) at the Faculty of Health Sciences, ULPGC, for the SEM images. The authors would like to thank Dr. Bernardino Clavo Varas, Head of the Research Unit at the Hospital Universitario de Gran Canaria Dr. Negrín for their technical assistance in conducting this study. We would also like to thank pharmacist Esther Artiles Ruano for her generous contribution to the materials used to collect blood samples and monitor blood glucose levels during this research.

Conflicts of Interest: The authors wish to declare that the patents have recently been licensed to an institutional spin-off without this fact influencing the interpretation of the results. The funders had no role in the design of the study; in the collection, analyses, or interpretation of data; in the writing of the manuscript; or in the decision to publish the results.

Abbreviations

The following abbreviations are used in this manuscript:

 doi:10.20944/preprints202506.0228.v1

PHVB	Poly (3-hydroxybutyrate-co-3-hydroxy valerate)
PHBV/AV	Poly (3-hydroxybutyrate-co-3-hydroxy valerate) /Aloe Vera
PHBV/Ho	Poly (3-hydroxybutyrate-co-3-hydroxy valerate)/Honey
PBS	Phosphate Buffer Saline
ECM	Extracellular matrix
PVA	Polyvinyl alcohol
PCL	Polycaprolactone
ULPGC	Universidad de Las Palmas de Gran Canaria.
FESEM	Field Emission Scanning Electron Microscope
UV	Ultraviolet
AIC	Akaike Information Criterion
SE	Standard Errors
SIMACE	Advanced Confocal and Electron Microscopy Research Facility

References

1. Hernández-Fuentes A., Cháves-Borges D., Cenobio-Galindo A., Zepeda-Velázquez A., Figuera A., Jiménez-Alvarado R., Campos-Montiel R. Characterization of total phenol and flavonoids contents, color, functional properties form honey samples with different floral origins. *Inter. J Food Stud*. 2021;(10):346–358 https://www.iseki-food-ejournal.com/ojs/index.php/e-journal/article/view/893/321
2. Jull A.B., Cullum N., Dumville J.C., Westby M.J., Deshpande S., Walker N. Honey as a topical wound treatment. *Cochrane Database Syst Rev*. 2015;2015(3):CD005083. doi:10.1002/14651858.CD005083.pub4
3. Merckoll P., Jonassen T., Vad M., Jeansson S., Melby K. Bacteria, biofilm, and honey: A study of the effects of honey on 'planktonic' and biofilm-embedded chronic wound bacteria. *Scand. J Infect. Dis.* 2009;41:341–347. https://doi.org/10.1080/00365540902849383
4. Miguel M., Antunes M., Faleiro M. Honey as a complementary medicine. *Integr. Med. Insights*. 2017;12:1–15. https://doi.org/10.1177/1178633717702869.
5. Pereira F., Bártolo, P. Traditional therapies for skin wound healing. *Adv. Wound Care*. 2016;5(5):208–229. https://doi.org/10.1089/wound.2013.0506. PMID: 27134765
6. Ruttermann M., Maier-Hasselmann A., Nink-Grebe B., Burckhardt M. Local treatment of chronic wounds. *Dtsch. Arztebl Int*. 2013;110(3):25–31. https://doi.org/10.3238/arztebl.2013.0025
7. Lee, S.K. Cell growth-stimulating effect. In: Park, Y.I., Lee, S.K. (eds) New Perspectives on Aloe. 2006. Springer, Boston, MA. https://doi.org/10.1007/0-387-34636-8_10.
8. Kumar R., Singh K., Gupta, A., Bishayee A., Pandey, A. Therapeutic potential of aloe vera-a miracle gift of nature. *Phytomedicine*. 2019;60, https://doi.org/10.1016/j.phymed.2019.152996
9. Lusby P., Coombes A., Wilkinson, J. (2002). Honey: A potent agent for wound healing? *J Wound Ostomy Continence Nurs. Soc*. 2002;29(6),295-300. https://doi.org/10.1067/mjw.2002.129073.
10. Mikołajczak, N. Potential health benefits of Aloe vera. *J Educ. Health Sport*. 2018;8(9):1420–1435. http://dx.doi.org/10.5281/zenodo.1434046.
11. Molan, P.C. The evidence supporting the use of honey as a wound dressing. *Int. J Low. Extrem. Wounds*. 2006;5(1):40–54. https://doi.org/10.1177/1534734605286014.
12. Song J.J., Salcido R. Use of honey in wound care: an update. *Adv. Skin Wound Care*. 2010:24(1):40–44, quiz 45–46. https://doi.org/10.1097/01.ASW.0000392731.34723.06
13. Ullah K., Naz S., Abudbos A. Towards a better understanding of the therapeutic applications and corresponding mechanisms of action of honey. *Environ. Sci. Pollut. Res*. 2017;24:27755–27766. https://doi.org/10.1007/s11356-017-0567-0
14. Yang X., Fan L., Ma L., Wang Y., Lin S., Yu F., Pan X., Luo G., Zhang D., Wang H. Green electrospun Manuka honey/silk fibroin fibrous matrices as a potential wound dressing. *Mater. Des*. 2017;119:76–84. DOI: 10.1016/j.matdes.2017.01.023]
15. Hernández-Rodríguez J., Martín-Barrasa J., Aragón-Sánchez J., Monzón-Mayor M., Pérez-Galván J., Saavedra-Santana P., Romero-Alemán M. The effect of honey, aloe vera, and hydrocolloid dressing on the healing process of murine excisional wounds. *Int. J Low. Extrem. Wounds*. 2023;22:1–9. Doi: 10.1177/15347346231214597

 doi:10.20944/preprints202506.0228.v1

16. Almasaudi, S. The antibacterial activities of honey. *Saudi J Biol. Sci*. 2021;28(4):2188–2196. doi:https://doi.org/10.1016/j.sjbs.2020.10.017.
17. Bucekova M., Buriova M., Pekarik L., Matjan V., Matjan J. Phytochemicals mediated hydrogen peroxide production is crucial for high antibacterial activity of honeydew honey. *Sci. Rep*. 2018;8:9061 https://doi.org/10.1038/s41598-018-27449-3.
18. González-Gascón R., Del Dedo-Torre P. Actualización sobre el uso de miel en el tratamiento de úlceras y heridas. Caso clínico. *Enferm. Glob.* 2004;4(1): 1–10. https://doi.org/10.6018/eglobal.3.1.577
19. Manjunatha D., Chua L. (2014). The anti-inflammatory and wound-healing properties of honey. *Eur. Food Res. Technol*. 2014;239(6):1003–1014. https://doi.org/10.1007/s00217-014-2297-6.
20. Weston R. The contribution of catalase and other natural products to the antibacterial activity of honey: A review. *Food Chem*. 2000;71(2):235–239. https://doi.org/10.1016/S0308-8146(00)00162-X.
21. Bucekova M, Jardekova L, Juricova V, et al. Antibacterial activity of different blossom honeys: new findings. *Molecules*. 2019;24(8):1573–1592. doi:10.3390/molecules24081573
22. Cianciosi D., Forbes-Hernández T.Y., Afrin S., et al. Phenolic compounds in honey and their associated health benefits: a review. *Molecules*. 2018;23(9):2322–2241. doi:10.3390/molecules23092322
23. Combarros-Fuertes P., Fresno J., Estevinho M., Sousa-Pimenta M., Tornadijo M., Estevinho, L. Honey: Another alternative in the fight against antibiotic resistant bacteria? *Antibiotics.* 2020;9(774):1–21. https://doi.org/10.3390/antibiotics9110774.
24. Da Silva P., Gauche C., Gonzaga L., Costa A., Felt R. Honey: Chemical composition, stability, and authenticity. *Food Chem*. 2016;196:309–323. https://doi.org/10.1016/j.foodchem.2015.09.051
25. Brudzynski K. A current perspective on hydrogen peroxide production in honey. A review. *Food Chem*. 2020;332:127229. doi:10.1016/j.foodchem.2020.127229
26. Kwakman P.H., Te Velde A.A., de Boer L., Vandenbroucke-Grauls C.M., Zaat S.A. Two major medicinal honeys have different mechanisms of bactericidal activity. *PLoS One*. 2011;6(3):e17709. doi:10.1371/journal.pone.0017709
27. Maddocks S., Jenkins, R. (2013). Honey: a sweet solution to the growing problem of antimicrobial resistance? *Future Microbiol*. 2013;8(11):1419–29. https://doi.org/10.2217/fmb.13.105
28. Masoura M., Gkatzionis K. The antimicrobial mechanism of Greek thyme honeys against methicillin-resistant *Staphylococcus aureus* clinical isolates: a case study of comparison with manuka honey. *Int. J of Food Sci. Tech.* 2022;57:7076–7084. doi: 10.1111/ijfs.16045
29. Yaghoobi R., Kazerouni A.,Kazerouni O. Evidence for clinical use of honey in wound healing as an anti-bacterial, anti-inflammatory, anti-oxidant and anti-viral agent: a review. *Jundishapur J. Nat. Pharm. Prod*. 2013;8(3):100–104. https://doi.org/10.17795/jjnpp-9487
30. Cosmetic Ingredient Review Expert Panel. Final report on the safety assessment of AloeAndongensis Extract, Aloe Andongensis Leaf Juice, Aloe arborescens Leaf Extract, Aloe Arborescens Leaf Juice, Aloe Arborescens Leaf Protoplasts, Aloe Barbadensis Flower Extract, Aloe Barbadensis Leaf, Aloe Barbadensis Leaf Extract, Aloe Barbadensis Leaf Juice, aloe Barbadensis Leaf Polysaccharides, Aloe Barbadensis Leaf Water, Aloe Ferox Leaf Extract, Aloe Ferox Leaf Juice, and Aloe Ferox Leaf Juice Extract. *Int. J. Toxicol*. 2007;26(Suppl 2):1–50. https://doi.org/10.1080/10915810701351186.
31. Chung M., Choi S. Wound healing effect. In: Park, Y.I., Lee, S.K. (eds). New Perspectives on Aloe. 2006. Springer, Boston, MA. https://doi.org/10.1007/0-387-34636-8_6
32. Hernández-Martínez F.J., Jiménez-Díaz J.F., Rodríguez de Vera B., Quintana-Montesdeoca M.P., Chacón-Ferrera R., Estévez-García M.L. (2010). Therapeutic use of Aloe Vera in pressure ulcers (PU).[El uso terapéutico del Aloe Vera en las úlceras por presión (UPP)]. Revista CENIC Ciencias Biológicas. 2020;41,1–4. https://www.redalyc.org/articulo.oa?id=181220509066
33. Kim, K.W. Angiogenic effect. In: Park, Y.I., Lee, S.K. (eds). New Perspectives on Aloe. 2006. Springer, Boston, MA. https://doi.org/10.1007/0-387-34636-8_7
34. Farzadinia P., Jofreh N., Khatamsaz S., Movahed A., Akbarzadeh S., Mohammadi M., Bargahi A. Anti-inflammatory and wound healing activities of aloe vera, honey, and milk ointment on second-degree burns in rats. *Int. J. Lower Extrem. Wounds*. 2016;15(3):241–247. https://doi.org/10.1177/1534734616645031

 doi:10.20944/preprints202506.0228.v1

35. Habeeb F., Satables G., Bradbury F., Nong S., Cameron P., Plevin R., Ferro V. (2007). The inner gel component of aloe vera suppresses bacterial-induced pro-inflammatory cytokines from human immune cells. *Methods*. 2007;42(4):388–393. https://doi.org/10.1016/j.ymeth.2007.03.005
36. Takzaree N., Hadjiakhndi A., Hassanzadeh G., Reza M., Manyi A., Majidi A. Transforming growth factor-β (TFG-β) activation in cutaneous wounds after topical application of aloe vera gel. *Can. J Physiol. Pharmacol*. 2016;94:1285–1290. https://doi.org/10.1139/cjpp-2015-0460
37. Choi S., Son B., Son Y., Park Y., Lee S., Chung M. (2001). The wound-healing effect of a glycoprotein fraction isolated from aloe vera. *Br J Dermato*. 2001;145(4): 535–545. https://doi.org/10.1046/j.1365-2133.2001.04410.x
38. Reynolds T., Dweck, A. (1999). Aloe vera leaf gel: a review update. *J Ethnopharmacol*. 1999;68(1-3):3–37. https://doi.org/10.1016/s0378-8741(99)00085-9
39. Lee I., Kwon H., Meng W., Kang K. Nanofabrication of microbial polyester by electrospinning promotes cell attachment. *Macromol. Res.* 2004;12:374–378.
40. Chen Q., Wu. The application of polyhydroxyalkanoates as tissue engineering materials. *Biomaterials.* 2005;26:6565–6578.
41. Romero-Alemán MM., Hernández-Rodríguez JE.,Pérez-Galván JM.,Monzón-Mayor,M. Hybrid electrospun PHBV/Aloe vera and PHBV/Honey nanofibers are scaffolds for rat dorsal root ganglion neurite outgrowth and guidance as well as for the regeneration of mouse skin after wounding. *Glia. 2019;* 67(sup.S1),p.E654-E655,AbstractT16-0048:124-125.
42. Romero-Alemán MD, Pérez-Galván JM, Hernández-Rodríguez JE, Monzón-Mayor M. The Potential of Aloe Vera in Solution and in Blended Nanofibers Containing Poly (3-Hydroxybutyrate-Co-3-Hydroxyvalerate) as Substrates for Neurite Outgrowth. *J Biomed Mater Res A*. 2025;113(1):e37825. doi:10.1002/jbm.a.37825
43. Masaeli E., Morshed M., Nasr-Esfahani M.H., et al. Fabrication, characterization, and cellular compatibility of poly(hydroxy alkanoate) composite nanofibrous scaffolds for nerve tissue engineering. *PLoS ONE. 2013;*8(2):e57157. doi:10.1371/journal.pone.0057157.
44. Satalkar P., Elger B., Shaw D. Defining nano, nanotechnology, and nanomedicine: Why should it matter? *Sci. Eng. Ethics*. 2016;22:1255–1276.
45. Chen W., Tong Y. PHBV microspheres as neural tissue engineering scaffolds support neuronal cell growth and axon–dendrite polarization. *Acta Biomaterialia*. 2012;8:540–548. https://doi.org/10.1016/j.actbio.2011.09.026
46. Prabhakaran M., Vatankhah E., Ramakrishna S. Electrospun aligned PHBV/collagen nanofibers as substrates for nerve tissue engineering. *Biotechnol. Bioeng*. 2013;110(10):2775–2784
47. Dumontel B, Conejo-Rodríguez V, Vallet-Regí M, Manzano M. Natural Biopolymers as Smart Coating Materials of Mesoporous Silica Nanoparticles for Drug Delivery. Pharmaceutics. 2023;15(2):447. Published 2023. doi:10.3390/pharmaceutics15020447
48. Jaldin-Crespo L., Silva N., Martínez J. Nanomaterials based on honey and propolis for wound healing—a mini-review. *Nanomaterials*. 2022;12:4409. https://doi.org/10.3390/nano12244409
49. Yupanqui M., Vyas C., Aslan E., Humphreys G., Diver C., Bartolo P. (2022) Honey: an advanced antimicrobial and wound healing biomaterial for tissue engineering applications. *Pharmaceutics*. 2022; 10,14(8):1663. doi: 10.3390/pharmaceutics14081663.
50. Rahman S., Carter P., Bhattarai N. Aloe vera for tissue engineering applications. *J Funct. Biomater.* 2017;8(1):6–22. doi:10.3390/jfb8010006
51. Thompson Z., Rahman S,. Yarmolenko S., Sankar J., Kumar D., Bhattarai N. Fabrication and characterization of magnesium ferrite-based PCL/Aloe vera nanofibers. *Materials (Basel)*. 2017;10(8):937–948. doi:10.3390/ma10080937
52. Shishatskaya E., Volova T., Puzyr A., Mogilnaya O., Efremov S. Tissue response to the implantation of biodegradable polyhydroxyalkanoate sutures. *J Mat. Sci. Mater. Med*. 2004;15(6):719–728. https://doi.org/10.1023/b:jmsm.0000030215.49991.0d.
53. Rubiano-Navarrete A.F., Rosas C. R. A., Torres P.Y., Gómez-Pachón E. Y. From fibers electrospun with honey to the healing of wounds: a review. *Ingeniería y competitividad*. 2024; *26*(2), e-30112811 https://doi.org/10.25100/iyc.v26i2.12811

 doi:10.20944/preprints202506.0228.v1

54. Davidson J., Yu F., Opalenik S. Splinting strategies to overcome confounding wound contraction in experimental animal models. *Adv Wound Care*. 2013; 2(4):142–148. https://doi.org/10.1089/wound.2012.0424.
55. Ren L., Zhou B., Chen L. (2012). Silicone ring implantation in an excisional murine wound model. *Wound*. 2012;24(2):36–42. PMID: 25876236
56. Ansell D., Campbell L., Thomason H., Brass A., Hardman M. A statistical analysis of murine incisional and excisional acute wound models. *Wound Rep. Reg*. 2014;22:281–287. https://doi.org/10.1111/WRR.12148.
57. Directive 2010/63/EU of the European Parliament and the Council. Official Journal of the European Union (2010).
58. Mukai K., Koike M., Nakamura S., et al. Evaluation of the effects of a combination of Japanese honey and hydrocolloid dressing on cutaneous wound healing in male mice. *Evid Based Complement Alternat Med*. 2015;2015:910605. doi:10.1155/2015/910605
59. Martins S., Torres O., Santos O., Limeira-Júnior A., Sauaia-Filho, E., Melo S., Santos, R., Silva V. Analysis of the healing process of the wounds occurring in rats using laser therapy associated with hydrocolloid. *Acta Ci.r Bras*. 2015;30(10):681–685. https://doi.org/10.1590/S0102-865020150100000005.
60. Takeuchi T., Ito M., Yamaguchi S., Watanabe S., Honda M., Imahashi T., Yamada T., Kokubo T. Hydrocolloid dressing improves wound healing by increasing M2 macrophage polarization in diabetic mice. *Nagoya J Med. Sci*. 2020;82(3):487–498. https://doi.org/10.18999/nagjms.82.3.487
61. Rasband W.S. ImageJ, U. S. National Institutes of Health, Bethesda, Maryland, USA, https://imagej.nih.gov/ij/, 1997-2018.
62. Molina A., Moyano M., Peña F., Lora A., Moreno S., Serrano, J. (2008). Central Nervous System depressants and anaesthesia in experimental rodents [Depresores del Sistema Nervioso Central y anestesia en roedores de experimentación]. *RECVET.2008;* 3(9). https://www.researchgate.net/publication/353849333_Depresores_del_Sistema_Nervioso_Central_y_anestesia_en_roedores_de_experimentacion_Central_Nervous_System_depressant_and_anaesthesia_of_Laboratory_rodents
63. Scepankova H., Combarros-Fuertes P., Fresno J.M., et al. Role of honey in advanced wound care. Molecules. 2021;26(16):4784. doi:10.3390/molecules26164784
64. Giusto G, Vercelli C, Comino F, Caramello V, Tursi M, Gandini M. A new, easy-to-make pectin-honey hydrogel enhances wound healing in rats. *BMC Complement Altern. Med*. 2017;17(1):266. doi:10.1186/s12906-017-1769-1
65. Monzón, M., Romero, M., Hernández,JE., Pérez,JM. Hybrid Aloe vera nanofibers. European Patent Office. EP 3461788;12.10:2022. Munich.
66. Monzón, M., Romero, M., Hernández,JE., Pérez,JM. Hybrid honey nanofibers. European Patent Office. EP 3428117;27.07:2022. Munich.
67. Yixiang, D., Yong, T., Liao, S., Chan, C. K., Ramakrishna, S2008. Degradation of electrospun nanofiber scaffold by short wave length ultraviolet radiation treatment and its potential applications in tissue engineering. *Tissue Eng*. Part A. 2008;14:1321–1329. https://doi.org/10.1089/ten.tea.2007.0395
68. Rasband, W.S., ImageJ, U. S. National Institutes of Health, Bethesda, Maryland, USA, https://imagej.nih.gov/ij/, 1997-2018.
69. Laird N.M., Ware J.H. Random-effects models for longitudinal data. *Biometrics*. 1982;38(4):963–974. PMID: 7168798 https://pubmed.ncbi.nlm.nih.gov/7168798/
70. Cavanaugh J., Neath A. The Akaike information criterion: Background, derivation, properties, application, interpretation, and refinements. WIREs *Comput Stat*. 2019;11:e1460. doi: https://doi.org/10.1002/wics.1460
71. R Development Core Team. R: a language and environment for statistical computing (Version 3.6.1). R Foundation for Statistical Computing, Vienna, Austria. 2019; https://www.R-project.org/.
72. Sosiati, H., Nur Fatihah, W., Yusmaniar, Nur Rahman, M.B., 2018. Characterization of the Properties of Electrospun Blended Hybrid Poly(Vinyl Alcohol)_Aloe Vera/Chitosan Nano-Emulsion Nanofibrous Membranes. KEM. https://doi.org/10.4028/www.scientific.net/kem.792.74
73. Van Zutphen L., Baumans V, Beynen A. Principles of Laboratory Animal Science, second edition, Elsevier Science, Amsterdam, 2001: https://www.humane-endpoints.info/es/rata/parametros-fisiologicos

 doi:10.20944/preprints202506.0228.v1

74. Rossiter K., Cooper A.J., Voegeli D., Lwaleed B.A. Honey promotes angiogenic activity in the rat aortic ring assay. *J Wound Care*. 2010;19(10):440–446. doi:10.12968/jowc.2010.19.10.79091
75. Sarkar S., Chaudhary A., Kumar S.T., Kumar D.A., Chatterjee J. Modulation of collagen population under honey-assisted wound healing in a diabetic rat model. Wound Medicine. 2018;20:7–17. https://doi.org/10.1016/j.wndm.2017.12.001
76. Andreu V., Mendoza G., Arruebo M., Irusta S. Smart dressings based on nanostructured fibers containing natural origin antimicrobial, anti-Inflammatory, and regenerative compounds. Materials (Basel). 2015;8(8):5154–5193. Published 2015 Aug 11. doi:10.3390/ma8085154
77. Maleki H., Gharehaghaji A, Dijkstra P. A novel honey-based nanofibrous scaffold for wound dressing application. *J Appl. Polym. Sci*. 2013;127:4086–4092. https://doi.org/10.1002/app.37601
78. Abrigo M., MacArthur S., Kingshott. Electrospun nanofibers as dressings for chronic wound care: advances, challenges, and prospects. *Macromol Biosci*. 2014;14:772–792. doi: 10.1002/mabi.201300561
79. Pilehvar-Soltanahmadi Y., Dadashpour M., Mohajeri A., Fattahi A., Sheervalilou R., Zarghami N. An overview on application of natural substances incorporated with electrospun nanofibrous scaffolds to development of innovative wound dressings. *Mini Rev. Med. Chem*. 2018;18(5):414–427. doi:10.2174/1389557517666170308112147
80. Suwantong O., Waleetorncheepsawat S., Sanchavanakit N., et al. In vitro biocompatibility of electrospun poly(3-hydroxybutyrate) and poly(3-hydroxybutyrate-co-3-hydroxyvalerate) fiber mats. *Int. J Biol. Macromol*. 2007;40(3):217–223. doi:10.1016/j.ijbiomac.2006.07.006
81. Sendil D., Gürsel I., Wise D.L., Hasirci V. Antibiotic release from biodegradable PHBV microparticles. *J Control Release*. 1999;59(2):207–217. doi:10.1016/s0168-3659(98)00195-3
82. Rahimnejad M., Derakhshanfar S., Zhong W. Biomaterials and tissue engineering for scar management in wound care. *Burns Trauma.* 2017; 5:4. Published 2017 Jan 21. doi:10.1186/s41038-017-0069-9
83. Gavillero-Martin A., Juliá-Roca M.,Serra-Guillén I., Rodríguez-Hernández A.,Manrique-Silva E.,López-Sundh A.E.,Nagore E. Secondary Intention healing time of postoperative surgical cancer skin wounds with a biosynthetic porcine type I collagen dressing: A 306-patient retrospective, observational study. *Actas Dermo-Sifiliográficas*.[In press]; 2024. https://doi.org/10.1016/j.ad.2025.02.022
84. Molina G. E., Sherry Y.H., Neel V. A. Observations Regarding Infection Risk in Lower-Extremity Wound Healing by Second Intention. *Dermatologic* Surgery.2020; 46(10):1342-1344. DOI: 10.1097/DSS.0000000000002094
85. Rodrigues M, Kosaric N, Bonham CA, Gurtner GC. Wound Healing: A Cellular Perspective. *Physiol Rev*. 2019; 99(1):665-706. doi:10.1152/physrev.00067.2017